Improved ENSO Prediction by Singular Vector Analysis in a Hybrid Coupled Model

XIAOBING ZHOU, YOUMIN TANG, YANJIE CHENG, AND ZIWANG DENG

Environmental Science and Engineering, University of Northern British Columbia, Prince George, British Columbia, Canada

(Manuscript received 6 September 2007, in final form 20 September 2008)

ABSTRACT

In this study, a method based on singular vector analysis is proposed to improve El Niño–Southern Oscillation (ENSO) predictions. Its essential idea is that the initial errors are projected onto their optimal growth patterns, which are propagated by the tangent linear model (TLM) of the original prediction model. The forecast errors at a given lead time of predictions are obtained, and then removed from the raw predictions. This method is applied to a realistic ENSO prediction model for improving prediction skill for the period from 1980 to 1999. This correction method considerably improves the ENSO prediction skill, compared with the original predictions without the correction.

1. Introduction

As an optimal perturbation method, singular vectors (SVs) have been widely applied in weather forecast and ENSO prediction, including the error-growth estimation and atmospheric predictability studies, the adaptive observation strategy, as well the construction of the initial fields for ensemble forecast (e.g., Lorenz 1965; Mureau et al. 1993; Penland and Sardeshmukh 1995; Xue et al. 1997a,b; Moore and Kleeman 1996, 2001; Moore et al. 2003; Fan et al. 2000; Tang et al. 2006; Zhou et al. 2007).

For any prediction system, there always exist initial uncertainties, even though data assimilation is applied. The optimal error growth, measured in the linear regime by the first singular value, gives an upper bound of possible forecast errors due to initial uncertainties. Even if initial errors are large enough to evolve into a nonlinear regime, the fastest-growing singular vectors are still of interest as a practical tool for the initialization of ensemble forecasts or error estimation (Fan et al. 2000). Lorenz (1965) first pointed out that the fastest error-growth rate, measured by the largest singular value of a tangent linear model (TLM), may vary by an order of magnitude due to changes in the initial system. Xue et al. (1997b) compared two initial conditions for the ENSO forecast in the Zebiak and Cane model (Zebiak and Cane 1987). They found that if the first singular vector components of the initial errors were removed from the old initial conditions, the forecast skill verified at the period between January 1972 and December 1992 was significantly improved. Yang et al. (2006) used a different optimal perturbation method—the bred vector (BV)—to estimate the growing forecast errors in the National Aeronautics and Space Administration (NASA) Seasonal-to-Interannual Prediction Project (NSIPP) global coupled model, and found that the BV is in very good agreement with the forecast error. In fact, the evolution of spatial structure of BV is similar to that of the final pattern of the leading singular vector during the prediction period in the coupled model (Cai et al. 2003). Recently, Mu and his collaborators proposed a new approach of error growth based on conditional nonlinear optimal perturbation (CNOP; Mu et al. 2003; Mu and Zhang 2006; Mu et al. 2007). The CNOP considers the nonlinear growth of errors and probably better characterizes the nonlinear nature of the real world.

In general, model prediction skills can be improved by refining model physical and dynamical processes as well using data assimilation. In this study, we propose an alternative scheme to improve prediction skill (i.e., using the SVs to estimate and then remove forecast errors from raw predictions). This method has not been addressed well in the field of prediction, since model development and data assimilation have been thought to be essential methods to improve the model skill. However,

Corresponding author address: Youmin Tang, Environmental Science and Engineering, University of Northern British Columbia, 3333 University Way, Prince George BC V2N 4Z9, Canada.
E-mail: ytang@unbc.ca

DOI: 10.1175/2008JTECHO599.1

this method might have practical significance, since the development of the model is complicated and difficult whereas the data assimilation has limitations such as the requirement of the exact representative of the background error covariance and a large observation coverage.

In our proposed scheme, the initial errors are obtained using the differences between the model simulation and the observations at the initial time. The error growth during the prediction period is obtained by the TLM of the original coupled model, and then removed from the original prediction. The method will be verified by a realistic ENSO forecast for the period from 1981 to 1999.

This paper is structured as follows: the coupled model is introduced in section 2, the method is described in section 3, the prediction results are presented in section 4, and a discussion and the conclusions can be found in section 5.

2. Description of coupled model and data

The ocean model used here for ENSO simulations and predictions is identical to that in Tang et al. (2001). It covers the tropical Pacific Ocean 30°N–30°S in latitude and 123°E–69°W in longitude with a horizontal resolution of 1.5° × 1.5°, and consists of the depth-averaged primitive equations in six layers (with reference thickness of 100, 175, 250, 320, 400, and 500 m from top to bottom).The time step is 2 h. The model allows for exchanges of mass, momentum, and heat at each layer interfaced by a parameterization of entrainment.

The atmospheric model used for ENSO predictions is an empirical statistic model by a nonlinear regression method—the neural network (NN). The wind stress is constructed using ocean states as predictors. The details of the oceanic and atmospheric model can be found in Tang et al. (2001) and Tang (2002).

The SST and the first-layer depth $\mathbf{H}_1$ in the ocean model play a major role for ENSO forecast (Tang and Kleeman 2002). The initial errors of predictions are defined as the difference between the model states and the observed counterpart; therefore, the observed SST and $\mathbf{H}_1$ are needed to obtain the initial errors. The SST observations used here are the Extended Reconstructed SST (ERSST) data (Smith and Reynolds 2003, 2004). Since the observed $\mathbf{H}_1$ data are not available currently, the proxy data of $\mathbf{H}_1$ have to be constructed.

The proxy $\mathbf{H}_1$ data are estimated using observed SST and observed wind stress. First, the ocean model is integrated for 28 yr from 1948 to 1975 forced by the National Centers for Environmental Prediction (NCEP) reanalysis wind data. A statistical relationship between model $\mathbf{H}_1$ and SST is derived using the singular value decomposition (SVD) technique. The first three SVD modes of $\mathbf{H}_1$ and SST are extracted. Tang and Kleeman (2002) used both methods—a linear regression (LR) and a nonlinear neural network—to build the relationship between modeled SST and $\mathbf{H}_1$. They found that the results were not sensitive to the linear or nonlinear hypotheses. Thus, the LR method is used here to estimate the proxy $\mathbf{H}_1$ data using SST observations.

3. Methodology

The ocean model is forced by the Florida State University (FSU) wind stress (Goldberg and O'Brien 1981) for 20 yr during the period from 1980 to 1999, which generates the initial conditions from which a set of prediction experiments is carried out. The proposed scheme of error correction is

$$T^c(x, y, t) = T^o(x, y, t) + \Delta T(x, y, t), \tag{1}$$

where $T^c(x, y, t)$ is the corrected prediction of SST, $T^o(x, y, t)$ is the original prediction of the SST, and $\Delta T(x, y, t)$ is the error. The zonal and meridional directions in space are x, y, and t is the lead time of prediction. The challenging issue here is how to compute the time-dependent error $\Delta T(x, y, t)$.

The variation of the eastern equatorial Pacific SST is mainly controlled by the advection of SST and by the $\mathbf{H}_1$ disturbance (Tang and Kleeman 2002). Denoting the initial errors in SST and in thermocline depth by $\Delta T(x, y, t_0)$ and $\Delta H(x, y, t_0)$, we define them as the difference between prediction and observation, namely,

$$\Delta T(x, y, t_0) = T^{\text{obs}}(x, y, t_0) - T(x, y, t_0), \tag{2}$$

$$\Delta H(x, y, t_0) = H^{\text{obs}}(x, y, t_0) - H(x, y, t_0), \tag{3}$$

where t_0 is initial time from which the prediction is started, $T^{\text{obs}}(x, y, t_0)$ and $H^{\text{obs}}(x, y, t_0)$ are observed SST and proxy $\mathbf{H}_1$ anomalies, and $T(x, y, t_0)$ and $H(x, y, t_0)$ are the model SST and $\mathbf{H}_1$ anomalies. The $\Delta T(x, y, t_0)$ and $\Delta H(x, y, t_0)$ are projected onto their leading singular vectors:

$$\Delta T'(x, y, t_0) = \sum_{i=1}^{2} \alpha_i \text{SV}_i^T(x, y), \tag{4}$$

$$\Delta H'(x, y, t_0) = \sum_{i=1}^{3} \beta_i \text{SV}_i^H(x, y), \tag{5}$$

where $\text{SV}_i^T(x, y)$ and $\text{SV}_i^H(x, y)$ are the ith singular vector of the model SST and $\mathbf{H}_1$. Here α_i and β_i are the projection coefficient of the initial errors in SST in (2)

and in $\mathbf{H}_1$ in (3), respectively, onto the ith singular vector, obtained by

$$\alpha_i = \sum_{x,y} \Delta T(x, y, t_0) \mathrm{SV}_i^T(x, y), \quad (6)$$

$$\beta_i = \sum_{x,y} \Delta H(x, y, t_0) \mathrm{SV}_i^H(x, y). \quad (7)$$

In this study, we take the first two SV modes for SST and the first three SV modes for $\mathbf{H}_1$, because they are only error-growing modes during the predictive period (i.e., singular values greater than 1).

The $\Delta T'(x, y, t_0)$ in (4) and $\Delta H'(x, y, t_0)$ in (5) are defined as the initial conditions of the TLM. With these initial conditions, the TLM can predict the evolution of the error growth and obtain the errors at any given lead time of predictions. As such the original predictions can be corrected by Eq. (1). We use the term *scheme 1* if we ignore the impact of initial uncertainties in $\mathbf{H}_1$ on SST; the term *scheme 2* is used when we consider the impact of the initial errors in both SST and $\mathbf{H}_1$ on the error growth of SST. For comparison we also perform a simple approach of initialization in this study, namely that, predictions are initialized by the observed SST and proxy $\mathbf{H}_1$ directly. This simple approach is called scheme 3.

The SVs used here were obtained by the TLM and its adjoint model (AM), which were developed by the online complier TAPENADE (more information available online at http://www-sop.inria.fr/tropics/). A Lanczos algorithm (Golub and Van Loan 1989) is used to select eigenvectors and eigenvalues. In this study, we use the Arnoldi Package (ARPACK) software package (Lehoucq et al. 1998) that was developed from the Lanczos algorithm to solve the singular value problem. The L_2 norm is used to calculate the SVs of SST and $\mathbf{H}_1$. The SVs' computation can be found in Zhou et al. (2007) in details.

The first singular vectors (SV1) of SST and $\mathbf{H}_1$ are shown in Fig. 1, computed starting from January 1982 at a 12-month optimization time. The corresponding reference state of the SVs is the model basic state obtained by the integration of the coupled model during the same period. It is clear to see that the SV1 of SST has a west–east dipole pattern spanned the tropical Pacific, which is similar to that of Chen et al. (1997) and Xue et al. (1997a), whereas the SV1 of $\mathbf{H}_1$ has the fastest error growth in the central western Pacific. The details of the SVs might depend on models used and norms defined, but the leading SV in this coupled model and other intermediate complexity models shows a common feature (i.e., a large-scale structure in the tropical Pacific and an insensitivity to the initial time and the length of optimization period; Zhou et al. 2007; Chen et al. 1997; Xue et al. 1997a; Fan et al. 2000, etc.). This allows us to use Fig. 1 to approximately represent the SVs starting from all initial conditions.

Figures 2 and 3 show the initial errors of SST and $\mathbf{H}_1$ on 1 July 1982 and 1 January 1988, respectively (top panels), the projection of the errors on the leading SVs pattern (middle panels), and the growth of the projected errors during a 12-month period by scheme 2 (bottom panels). A strong El Niño event occurred in 1982/83 whereas a large La Niña event appeared in 1988. For SST, the projections of the raw errors on the leading singular vectors (Figs. 2b and 3b) can explain 55% and 44% of total initial errors (Figs. 2a and 3a versus 2b and 3b).[1] For $\mathbf{H}_1$, 82% and 42% of the original initial errors can be explained by the leading SV modes (Figs. 2d and 3d versus Figs. 2e and 3e).

Figures 2c and 3c show that the model initial SST errors in the Niño-3 (5°S–5°N, 150°–90°W) and Niño-4 (5°S–5°N, 160°E–150°W) have faster growth during the strong El Niño period than during the La Niña event. This result is consistent with that found in Moore and Kleeman (1996), which showed the error growth to be enhanced during the onset of El Niño and suppressed during the onset of La Niña. For $\mathbf{H}_1$ errors, the amplitude of final errors is at the same order of that of initial errors in both Figs. 2 and 3, suggesting that the error growth of $\mathbf{H}_1$ is not as fast as that of SSTA. The projected errors on the SST SV1 are mainly located in the central equatorial Pacific, as shown in Figs. 2b and 3b. This indicates that the initial uncertainty of SST in the central equatorial Pacific is most favored to the growth of SST anomaly (SSTA) prediction errors. This is consistent with previous results found in other ENSO models such as Xue et al. 1997a, Chen et al. 1997, and Tang et al. 2006.

Figures 2d–f and 3d–f describe $\mathbf{H}_1$ initial errors, its projection on $\mathbf{H}_1$ SV1, and the final pattern for the two ENSO events, respectively. As can be seen, the large anomalous centers in these figures are not located in the central equatorial Pacific. It is due mainly to the definition of SV norm in this study and the process inherent to ENSO dynamics. In scheme 2, the norm of the error growth is defined by the equatorial Pacific SSTA, thereby Figs. 2e and 3e indicate where $\mathbf{H}_1$ is the most favorable to the equatorial Pacific SSTA error growth (mostly controlled by the Niño-3.4 SSTA error growth; Tang et al. 2006), whereas Figs. 2f and 3f indicate how the initial uncertainty in $\mathbf{H}_1$ evolves corresponding with

[1] Denoted by $x(i, j)$ and $y(i, j)$ the value of grid point (i, j) in Figs. 2 and 3; R, the ratio of projection of initial errors on the leading SV to the raw errors, is defined by $R = \sum_i \sum_j |y(i,j)| / \sum_i \sum_j |x(i,j)|$, i, j over the whole model domain.

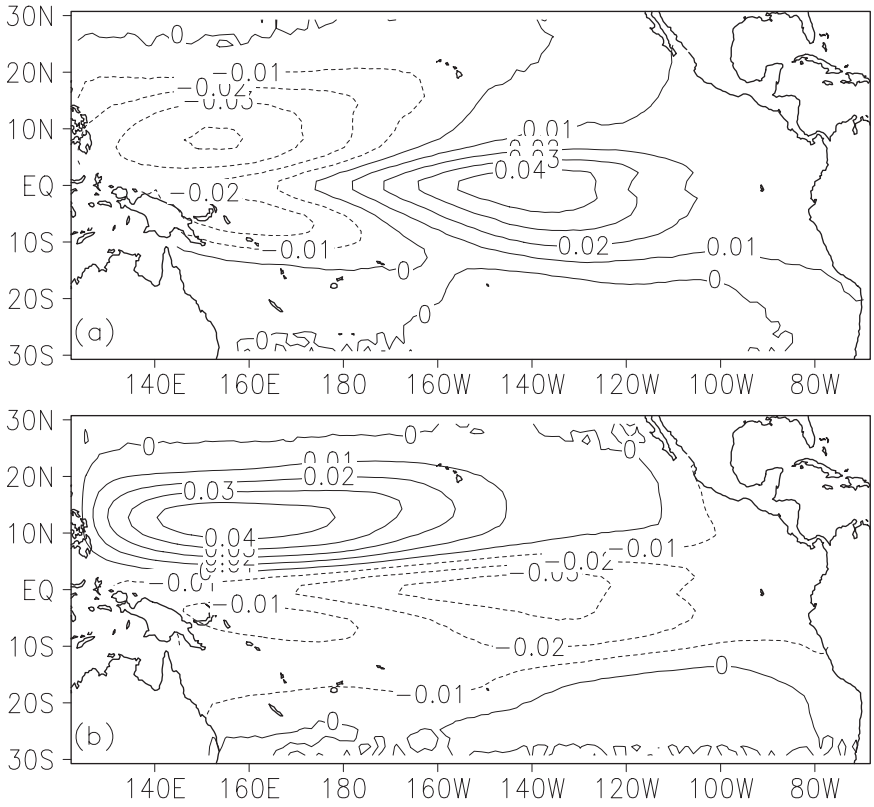

FIG. 1. SV1 starting in January 1982 at the optimization time of 12 months. (a) SV1 of SST (°C) and (b) the first-layer depth (m). Their corresponding singular values are 3.95 and 4.89, respectively.

the fastest growth of prediction errors of the equatorial SSTA. In this model, $\mathbf{H}_1$ is nearly equivalent to the thermocline depth. Based on the delay-oscillator mechanism, the dynamical basis of the ENSO cycle in this model (Tang 2002), the thermocline disturbance in the off-equatorial western Pacific plays a very important role in dominating and influencing ENSO simulation and prediction. This explains why Figs. 2e,f and 3e,f have significant amplitude centers in the off-equatorial regions, rather than in the Niño-3.4 region itself. Since a lagged relationship always exists between the variation of the thermocline in the western Pacific and SSTA variability in Niño-3.4 region as evidenced in observations and modeling (e.g., Tang 2002; Latif and Flugel 1991), the thermocline disturbance is an effective precursor of ENSO prediction. Thus, the correction to the $\mathbf{H}_1$ errors of an earlier stage can significantly improve ENSO prediction skills of several months later. This is consistent with Fig. 4 where the consideration of the initial errors of $\mathbf{H}_1$ can lead to an improvement of the ENSO prediction over 6-month leads.

It should be noticed that the initial errors in $\mathbf{H}_1$ have a significant impact on ENSO prediction. The final SST error growth of 12-month leads in scheme 2 reaches up to 1.8°C as seen in Fig. 2c, against 0.35°C of scheme 1 where the initial errors of $\mathbf{H}_1$ are not considered (not shown). Therefore, an important issue in ENSO prediction is to assimilate subsurface oceanic observations or sea level height as evidenced in the initialization schemes of almost all ENSO predictions.

4. Implication of the correction scheme

In this section, we will examine the proposed schemes via realistic ENSO prediction from 1980 to 1999. The prediction is performed every 3 months, starting on 1 January, 1 April, 1 July, and 1 October, and lasts for 12 months.

Figures 4a,b show the correlation and root-mean-square error (RMSE) skill of the predictions, where the predicted Niño-3.4 SSTA is compared against the observed counterpart. As can be seen, the prediction skills without correction rapidly decline with lead times. The correlation decreases to 0.46 at the 12-month lead. At the lead times within 6 months, the prediction skills of scheme 1 are higher than those of the original prediction.

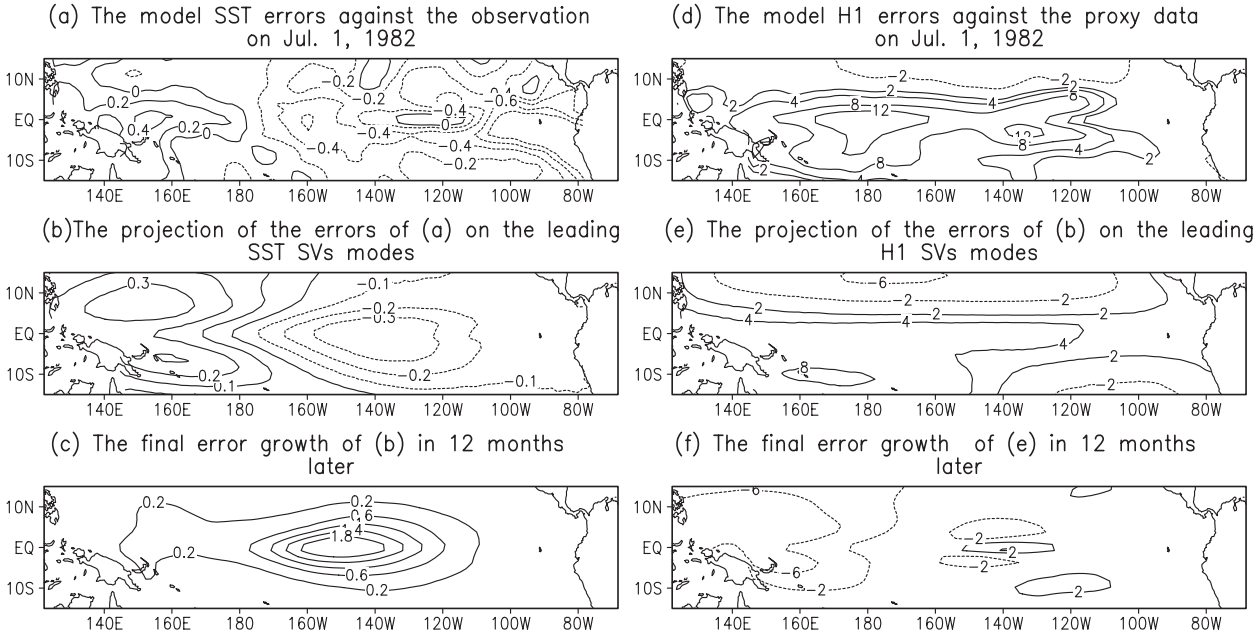

FIG. 2. (a),(b),(c) Several errors of model SST (°C) and (d),(e),(f) model $\mathbf{H}_1$ (m) for 1 Jul 1982. (a),(d) The raw errors measured by the difference between the observation and model; (b),(e) the projection of the raw errors on the leading singular vectors; and (c),(f) the growth of these projected errors at a 12-month lead by scheme 2.

However, at the lead times beyond 8 months, they are even lower than those without correction. Scheme 2 has the best prediction skills, with a correlation of greater than 0.6 for all lead times. Schemes 1 and 2 have almost the same prediction skills at lead times within 6 months. The prediction skills of scheme 1 continuously decrease with lead times beyond 6 months, whereas those of scheme 2 are stable and even rebound until a lead time of 12 months. In scheme 1, the SST error growth is considered to be due to only the initial errors in SST;

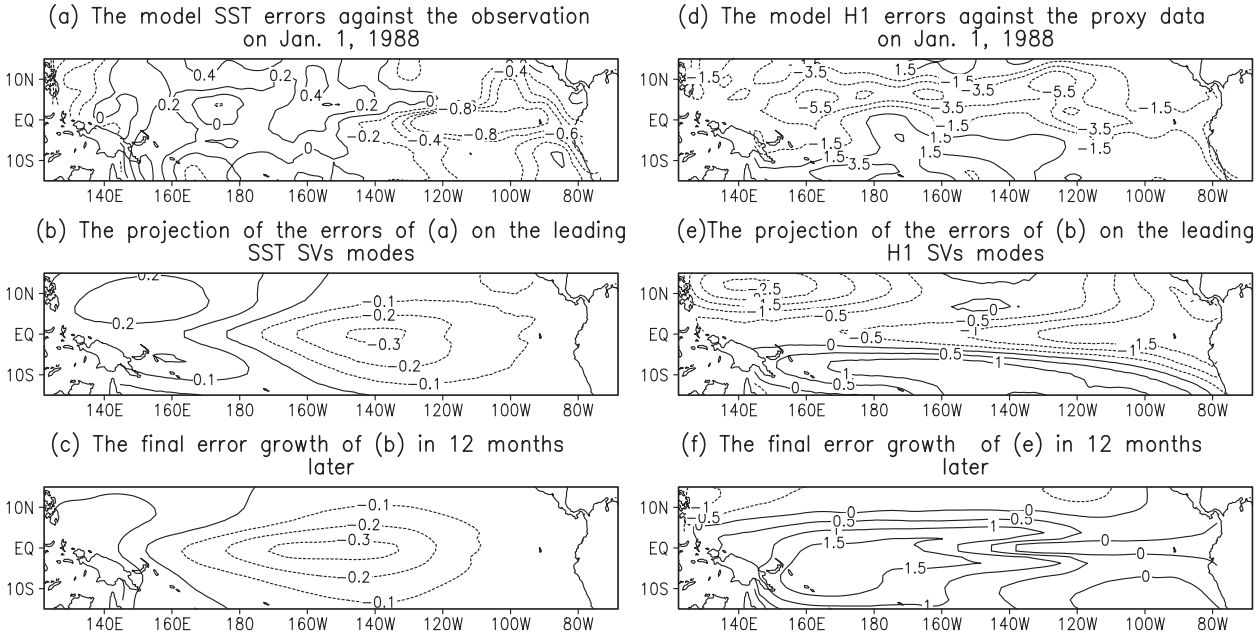

FIG. 3. As in Fig. 2, but for the 1988 cold event.

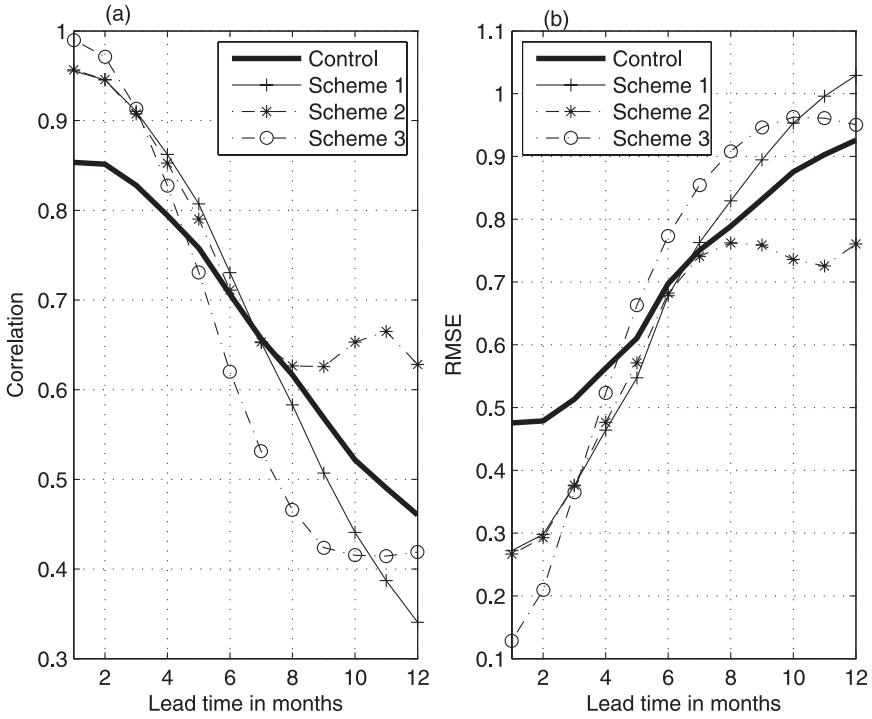

FIG. 4. (a) Correlation and (b) RMSE between observed and predicted SSTA Niño-3.4 index as a function of lead time. The predictions are initialized every 3 months from 1980 to 1999. The "control" denotes the original prediction without corrections. Scheme 1 only considers the initial errors in SST; both errors of SST and the first-layer depth are considered in scheme 2; and scheme 3 used SST observation and the proxy $\mathbf{H}_1$ data directly to initialize predictions.

whereas in scheme 2, the impact of H1 inital errors on prediction errors is also considered. Figure 4 suggests that the initial errors in SST control the prediction error growth during the first 6 months, beyond which the prediction errors are mainly determined by the initial errors in the first-layer depth. The improvement in the RMSE by scheme 2 is consistent with that in the correlation. At a 12-month lead, the RMSE in original prediction is 0.92, but is reduced to 0.76 by scheme 2. These results indicate that the $\mathbf{H}_1$ errors strongly impact the growth of SST error beyond 6-month leads, as discussed in the previous section. Scheme 3 has the best prediction skills at the first 2-month leads, beyond which the skill decreases rapidly, and is much lower than the skill initialized from the control run after 5-month leads. This is due probably to the model "shock" since noisy observations are inserted into the model directly. On the other hand, schemes 1 and 2 proposed in this study are performed in an "offline" strategy (i.e., correcting prediction through removing growth errors from raw predictions).

Figure 5 shows the variation of predicted Niño-3.4 from 1980 to 1999, at the lead time of 3 and 10 months, respectively. It is found that scheme 2 has the best predictions for ENSO events, particularly in the phase prediction. The phase delay that appears in the original prediction and scheme 1 is much alleviated in scheme 2. As can be seen, scheme 2 can predict most El Niño events well during 1980–99 such as 1982/83, 1986/87, and 1993/94 in both amplitudes and phases. One exception is the correction to the prediction of the 1997/98 event at the lead time of 12 months, in which scheme 2 leads to a weaker amplitude of the prediction compared with that in the original prediction and in scheme 1. We are not clear why scheme 2 is not working well with this specific case when it is good for all other predictions. One probable explanation is that the proxy $\mathbf{H}_1$ observation data cannot be estimated very realistically by the statistical relationship for the strongest ENSO event in the last century. Often the statistical relationship does not hold well for extreme cases (Gerstengarbe and Werner 1991).

It should be noticed that both schemes 1 and 2 have better improvement in the predictions of warm events than those in cold events. One can naturally speculate that this is probably due to using the SVs of warm events for correcting all predictions. To examine the possible impact of SVs on prediction improvement, we chose

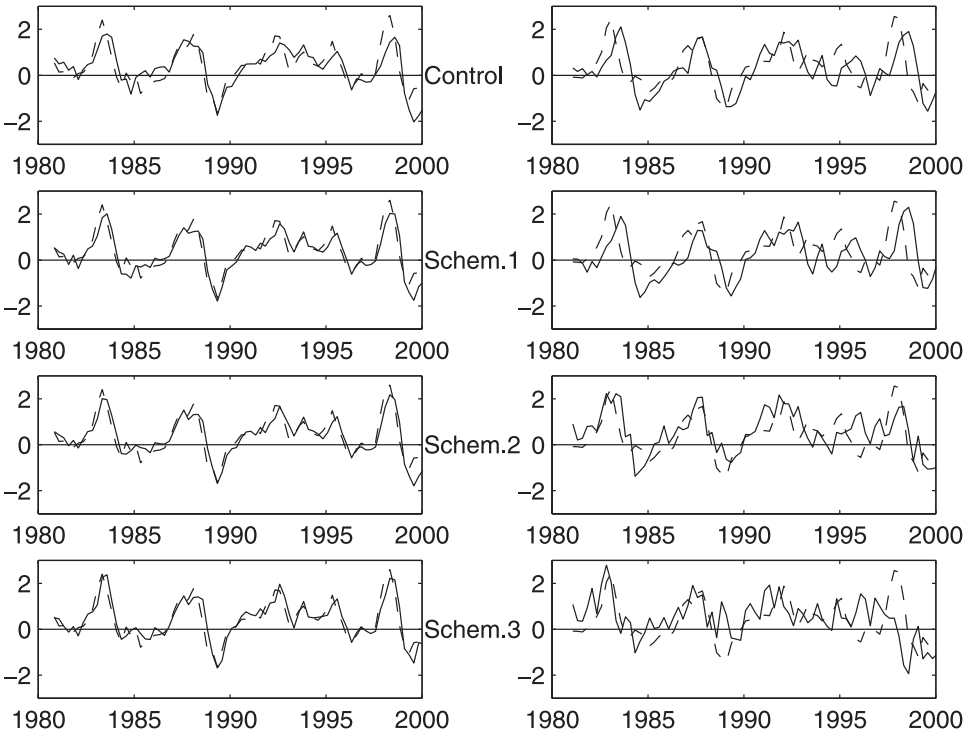

FIG. 5. The predicted Niño-3.4 SSTA (solid line) at the lead times of (left) 3 and (right) 10 months from 1980 to 1999. The observed Niño-3.4 index is also shown in the dashed line (°C).

singular vectors initialized from other several phases such as a neural state or a strong La Niña event (1988) to correct predictions. The results showed that the improvements in prediction skills are similar to those reported above (not shown). This is because the leading SVs are not sensitive to initial conditions as discussed before. A comparison between Figs. 2 and 3 reveals that the larger error growth characterized by SVs occurs in the 1982/83 El Niño event rather than in the 1988 La Niña event. Thus, the correction schemes proposed in this study are probably more effective for the predictions of warm events.

5. Discussion and conclusions

ENSO prediction is one of key issues in ENSO study. It can be improved by developing coupled models and data assimilation systems. A hierarchy of coupled atmosphere–ocean models has been developed since the 1980s. These models range from intermediate couple models to coupled general circulation models (e.g., Barnston et al. 1999; Kirtman et al. 2002, etc.). Many methods of data assimilation have also been explored such as the variational method and the Kalman filter. In this study, we proposed an alternative method to improve the ENSO dynamical prediction, in which the error growth of prediction is measured and then removed from the raw prediction. This method was applied to a realistic ENSO prediction model, and verified using the prediction of Niño-3.4 SSTA index from 1980 to 1999. The results show that the proposed method can lead to considerable improvements in the ENSO prediction skill. If the prediction error growth is considered only due to the initial errors in SST, the improvement of the prediction skill is valid until a 6-month lead; whereas when the prediction error growth is considered due to the initial errors in both SST and the first-layer depth, the proposed method is effective for the prediction until a 12-month lead time.

One key point in this method is to project initial errors on the leading singular vectors. This produces the initial error pattern that leads to the optimal growth of prediction errors. We also tested another simple correction method of errors that is sometimes used in ENSO prediction, in which the initial errors persisted through the prediction period and removed from the raw prediction. With this simple method, we found that the corrected skill in our model significantly degrades with lead times, even worse than in scheme 1. Actually, the simple scheme is a specific case of our proposed method.

In this study, we did not use the observed data of the first-layer depth to estimate its initial errors due to low resolution in the ocean model. Instead, we proposed the proxy $\mathbf{H}_1$ observation data for obtaining the initial errors of the first-layer depth. Obviously, this will lead to considerable uncertainties in the estimate of the initial errors, which impacts the correction of prediction errors. Even in this case, however, this method still brings considerable improvements in prediction skills for the hybrid model. Thus, one can reasonably assume that the proposed method can probably lead to more significant improvements in ENSO predictions for higher-resolution models.

It should be noticed that the SVs used here are calculated starting from a specified time, 1 January 1982, at a 12-month optimization time. We also used SVs starting from other times such as a neutral state to verify scheme 2. The results are similar to those reported above (not shown).

In this study, the prediction errors are estimated using SVs that only consider the linear growth of errors. As mentioned in the introduction, a new approach of error growth, CNOP, has been proposed in the nonlinear regime (Mu et al. 2003; Mu and Zhang 2006; Mu et al. 2007). It was found that CNOP tended to evolve into El Niño or La Niña events more probably than linear SV on the condition that CNOP and linear SV are of the same magnitude of norm (Mu et al. 2003). Therefore, if the CNOP-type errors are measured and then removed from raw predictions, the better skills of predictions might be able to be realized.

Acknowledgments. This work was supported by the Canadian Foundation for Climate and Atmospheric Sciences Grant GR-523 to Y. Tang.

REFERENCES

Barnston, A. G., M. H. Glantz, and Y. He, 1999: Predictive skill of statistical and dynamical climate models in forecasts of SST during the 1997–98 El Niño episode and the 1998 La Niña onset. *Bull. Amer. Meteor. Soc.,* **80,** 217–244.

Cai, M., E. Kalnay, and Z. Toth, 2003: Bred vectors of the Zebiak–Cane model and their application to ENSO predictions. *J. Climate,* **16,** 40–56.

Chen, Y.-Q., D. S. Battisti, T. N. Palmer, J. Barsugli, and E. S. Sarachik, 1997: A study of the predictability of tropical Pacific SST in a coupled atmosphere–ocean model using singular vector analysis: The role of the annual cycle and the ENSO cycle. *Mon. Wea. Rev.,* **125,** 831–845.

Fan, Y., M. R. Allen, D. L. T. Anderson, and M. A. Balmaseda, 2000: How predictability depends on the nature of uncertainty in initial conditions in a coupled model of ENSO. *J. Climate,* **13,** 3298–3313.

Gerstengarbe, F.-W., and P. C. Werner, 1991: Some critical remarks on the use of extreme-value statistics in climatology. *Theor. Appl. Climatol.,* **44,** 1–8.

Goldberg, S. D., and J. J. O'Brien, 1981: Time and space variability of tropical Pacific wind stress. *Mon. Wea. Rev.,* **109,** 1190–1207.

Golub, G. H., and C. F. Van Loan, 1989: *Matrix Computations*. 2nd ed. Johns Hopkins University Press, 664 pp.

Kirtman, B. P., Y. Fan, and E. K. Schneider, 2002: The COLA global coupled and anomaly coupled ocean–atmosphere GCM. *J. Climate,* **15,** 2301–2320.

Latif, M., and M. Flugel, 1991: An investigation of short-range climate predictability in the tropical Pacific. *J. Geophys. Res.,* **96,** 2661–2673.

Lehoucq, R. B., D. C. Sorensen, and C. Yang, 1998: ARPACK users' guide. SIAM, Philadelphia, PA, 142 pp.

Lorenz, E. N., 1965: A study of the predictability of a 28-variable atmospheric model. *Tellus,* **17,** 321–333.

Moore, A. M., and R. Kleeman, 1996: The dynamics of error growth and predictability in a coupled model of ENSO. *Quart. J. Roy. Meteor. Soc.,* **122,** 1405–1446.

——, and ——, 2001: On the differences between the optimal perturbations of coupled models of ENSO. *J. Climate,* **14,** 138–163.

——, J. Vialard, A. T. Weaver, D. L. T. Anderson, R. Kleeman, and J. R. Johnson, 2003: The role of air–sea interaction in controlling the optimal perturbations of low-frequency tropical coupled ocean–atmosphere modes. *J. Climate,* **16,** 951–968.

Mu, M., and Z. Zhang, 2006: Conditional nonlinear optimal perturbations of a two-dimensional quasigeostrophic model. *J. Atmos. Sci.,* **63,** 1587–1604.

——, W. Duan, and B. Wang, 2003: Conditional nonlinear optimal perturbation and its applications. *Nonlinear Processes Geophys.,* **10,** 493–501.

——, H. Xu, and W. Duan, 2007: A kind of initial error related to ''spring predictability barrier'' for El Niño events in the Zebiak–Cane model. *Geophys. Res. Lett.,* **34,** L03709, doi:10.1029/2007GL027412.

Mureau, R., F. Molteni, and T. N. Palmer, 1993: Ensemble prediction using dynamically conditioned perturbations. *Quart. J. Roy. Meteor. Soc.,* **119,** 299–323.

Penland, C., and P. Sardeshmukh, 1995: The optimal growth of tropical sea surface temperature anomalies. *J. Climate,* **8,** 1999–2024.

Smith, T. M., and R. W. Reynolds, 2003: Extended reconstruction of global sea surface temperatures based on COADS data (1854–1997). *J. Climate,* **16,** 1495–1510.

——, and ——, 2004: Improved extended reconstruction of SST (1854–1997). *J. Climate,* **17,** 2466–2477.

Tang, Y., 2002: Hybrid coupled models of the tropical Pacific–interannual variability. *Climate Dyn.,* **19,** 331–342.

——, and R. Kleeman, 2002: A new strategy for assimilating SST data for ENSO predictions. *Geophys. Res. Lett.,* **29,** 1841, doi:10.1029/2002GL014860.

——, W. W. Hsieh, B. Tang, and K. Haines, 2001: A neural network atmospheric model for hybrid coupled modelling. *Climate Dyn.,* **17,** 445–455.

——, R. Kleeman, and S. Miller, 2006: ENSO predictability of a fully coupled GCM model using singular vector analysis. *J. Climate,* **19,** 3361–3377.

Xue, Y., M. A. Cane, and S. E. Zebiak, 1997a: Predictability of a coupled model of ENSO using singular vector analysis. Part I:

Optimal growth in seasonal background and ENSO cycles. *Mon. Wea. Rev.,* **125,** 2043–2056.

——, ——, and ——, 1997b: Predictability of a coupled model of ENSO using singular vector analysis. Part II: Optimal growth and forecast skill. *Mon. Wea. Rev.,* **125,** 2057–2073.

Yang, S.-C., M. Cai, E. Kalnay, M. Rienecker, G. Yuan, and Z. Toth, 2006: ENSO bred vectors in coupled ocean–atmosphere general circulation models. *J. Climate,* **19,** 1422–1436.

Zebiak, S. E., and M. A. Cane, 1987: A model El Niño–Southern Oscillation. *Mon. Wea. Rev.,* **115,** 2262–2278.

Zhou, X., Y. Tang, and Z. Deng, 2007: The impact of atmospheric nonlinearities on the fastest growth of ENSO prediction error. *Climate Dyn.,* **30,** 519–531, doi:10.1007/s00382-007-0302-5.